Aalborg Universitet

AALBORG UNIVERSITY
DENMARK

Beam-Steerable Multi-Band Mm-Wave Bow-Tie Antenna Array for Mobile Terminals

Rodriguez Cano, Rocio; Zhang, Shuai; Pedersen, Gert F.

Published in:
2018 IEEE 12th European Conference on Antenna and Propagation (EuCAP)

DOI (link to publication from Publisher):
10.1049/cp.2018.0418

Publication date:
2018

Document Version
Accepted author manuscript, peer reviewed version

Link to publication from Aalborg University

Citation for published version (APA):
Rodriguez Cano, R., Zhang, S., & Pedersen, G. F. (2018). Beam-Steerable Multi-Band Mm-Wave Bow-Tie Antenna Array for Mobile Terminals. In *2018 IEEE 12th European Conference on Antenna and Propagation (EuCAP)* Institution of Engineering and Technology. https://doi.org/10.1049/cp.2018.0418

General rights
Copyright and moral rights for the publications made accessible in the public portal are retained by the authors and/or other copyright owners and it is a condition of accessing publications that users recognise and abide by the legal requirements associated with these rights.

- Users may download and print one copy of any publication from the public portal for the purpose of private study or research.
- You may not further distribute the material or use it for any profit-making activity or commercial gain
- You may freely distribute the URL identifying the publication in the public portal -

Take down policy
If you believe that this document breaches copyright please contact us at vbn@aub.aau.dk providing details, and we will remove access to the work immediately and investigate your claim.

Downloaded from vbn.aau.dk on: May 04, 2023

Beam-Steerable Multi-Band Mm-Wave Bow-Tie Antenna Array for Mobile Terminals

Rocío Rodríguez-Cano, Shuai Zhang, Gert F. Pedersen
Antenna, Propagation and Mm-Wave Systems Section (APMS), Department of Electronic Systems,
Aalborg University, Aalborg, Denmark
{*rrc,sz,gfp*}*@es.aau.dk*

***Abstract*—A multiple-band 5G end-fire antenna array is proposed to be placed on the upper and bottom edges of mobile terminals. The antenna element consists of two bow-tie radiators designed to resonate at 28 and 60 GHz. A sixteen-element beam-steerable array is presented in this paper, with overall dimensions of 40.13×1.44×0.25 mm^3. Only the odd elements are active in the 28-GHz band and the optimal termination of the parasitic elements is studied. The simulated results show a good match to a 50-ohm feeding line and end-fire radiation at the targeted frequency bands.**

***Index Terms*— mobile antenna, millimeter wave, dual band, beam steering.**

I. Introduction

The exponential growth of capacity demand and data rates in mobile communications can only be achieved by relocating the operating bands to higher frequencies. The bands around 28 GHz and 60 GHz are candidates for the upcoming fifth generation (5G). To compensate the higher propagation losses when the frequency increases, high gain antennas are required. For this reason, arrays are embedded in phone terminals to overcome the reception of low signal levels [1].

Several multi-band antennas have been proposed in the millimeter-wave (mm-wave) frequencies. In [2], a star-shaped patch antenna array is designed for UAV applications. The operating bands are $29-30$ GHz and $57-66$ GHz, and the dimensions of the unit cell are 9.5×9.5 mm^2. A dual-band (28 and 38 GHz) circularly polarized slotted patch antenna is studied in [3]. The size of the element is 6.8×6.8 mm^2. In [4], a dual-polarized capped bow-tie antenna is proposed to perform as a dual-band, dual-polarized array antenna at 23 GHz and at $70-85$ GHz. The overall dimensions of the element are $1.89\times1.89\times1.46$ mm^3. Nevertheless, the antennas presented in the aforementioned papers are not designed to cover the frequencies of 28 and 60 GHz.

Moreover, the total volume of these antennas is too big to be embedded in a mobile terminal. Bow-tie-shaped elements are attractive candidates for applications where the size is a constraint since they can be seen as the combination of two triangular patches instead of the traditional rectangular-shaped one. Besides, the bow-tie geometry also reduces the length of the conventional monopole antennas [5].

Linear arrays have been widely studied in the bibliography. In order to avoid grating lobes in a uniform linear array with end-fire radiation, the spacing between elements should be less than $\lambda/2$ [6]. For a wide-band or multi-band mm-wave array, the spacing should be fixed by the highest operating frequency. When the array works at the low mm-wave frequencies, the inter-element distance becomes electrically smaller. This leads to strong mutual coupling between elements and the reduction of radiation efficiency. In this case, it is better to only activate the even or odd number of elements in the whole linear array. The port termination of the non-activated elements has to be carefully investigated.

In this manuscript, the design of a low-profile double bow-tie array for 5G-enabled mobile terminals is carried out. Antenna candidates for handsets are required to be fitted in small areas, and the proposed antenna only occupies a clearance of 1.44 mm. At 28 GHz, when only the even antenna elements are excited, a study of the effect of the port termination in terms of impedance matching, scanning properties, and radiation efficiency is presented. The scanning behaviour of the array when all the elements are active is shown at 60 GHz and at the parasitic resonance frequencies.

II. Antenna Geometry and Analysis

A. Antenna Description

The configuration of the unit element of the array is shown in Fig. 1. The antenna consists of two antipodal bow-tie-shaped geometries designed to operate at 28 and 60 GHz, fed by a microstrip line. The substrate presents a dielectric constant of $\epsilon_r = 16$ and a thickness of 0.25 mm. The geometry has overall dimensions of $2.63 \times 1.44 \times 0.25$ mm^3.

The design parameters of the optimised antenna are given in Table I. The chosen opening angle of both bow-tie geometries is 22°.

Parameter	Value (mm)	Parameter	Value (mm)
L_{gnd}	0.22	L_2	0.31
W_{gnd}	2.63	R_1	0.76
L_1	0.35	R_2	0.28
W_1	0.11	R_3	0.26

TABLE I
Design parameters

B. Results

In order to model the boundary conditions, the antenna has been simulated with two parasitic antennas, one on the left and

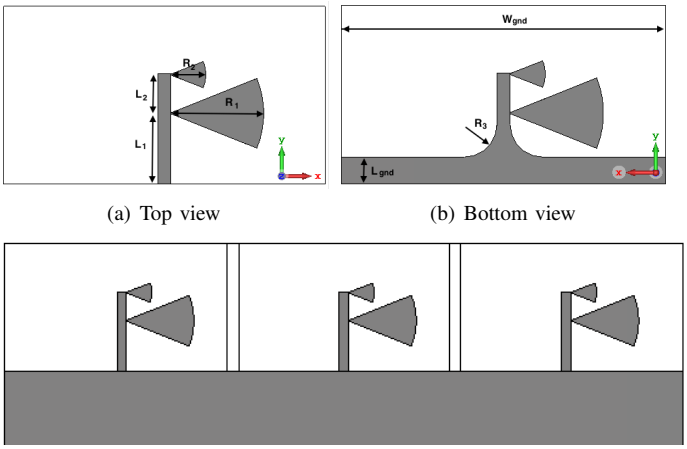

(a) Top view (b) Bottom view

(c) Antenna with boundaries

Fig. 1. Main element topology.

another one on the right, and with a portion of the phone PCB, as shown in Fig. 1c. The simulations are performed with the aid of the full-wave electromagnetic solver CST Microwave Studio.

Fig. 2 shows the reflection coefficient of the central antenna. The structure is matched below -10 dB at 28 GHz and at the band between 58 GHz and 70 GHz. Two parasitic resonances have appeared at 38 and 48 GHz due to the coupling between adjacent elements.

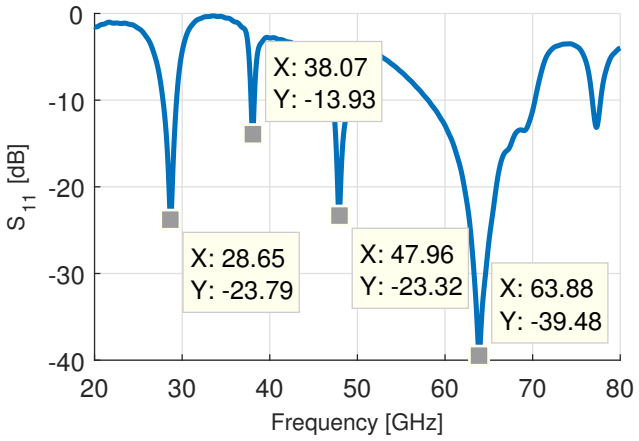

Fig. 2. Reflection coefficient of the antenna element.

The $\theta = 90°$ cut of the radiation pattern of the antenna at the two designed frequency bands is illustrated in Fig. 3. The orientation of the coordinate system is shown in Fig. 1, and only the central element is excited. The double bow-tie shows good end-fire radiation at the two bands. The gain of the antenna at boresight is 3.5 and 4.6 dBi for 28 and 60 GHz, respectively.

The radiation pattern at the parasitic resonance frequencies of 38 GHz and 48 GHz is shown in Fig. 4. As further detailed in Section III-B, at 38 GHz the radiation pattern is not end-fire

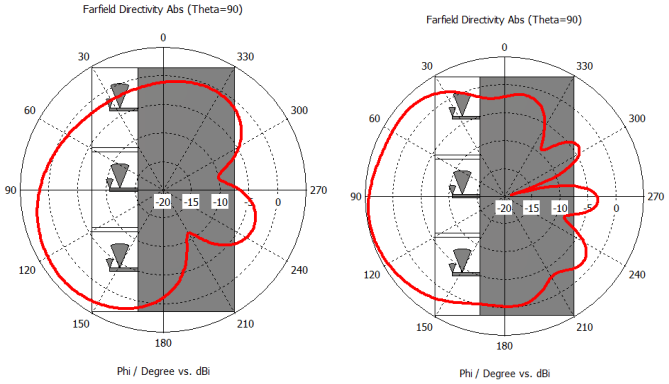

(a) 28 GHz (b) 60 GHz

Fig. 3. Radiation pattern of the antenna ($\theta = 90°$ cut) at the designed frequencies.

anymore. The directivity at these two frequencies is 5.5 and 4.2 dBi.

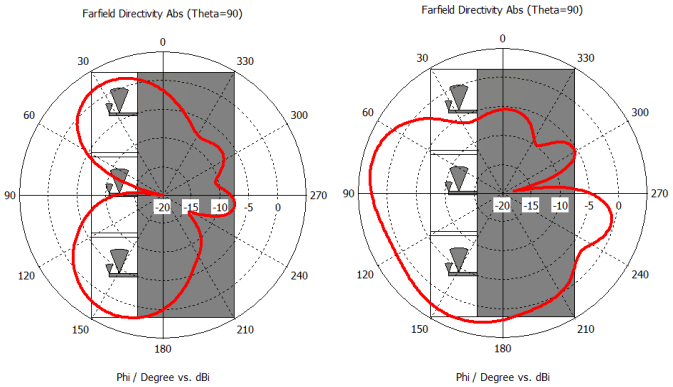

(a) 38 GHz (b) 48 GHz

Fig. 4. Radiation pattern of the antenna ($\theta = 90°$ cut) at the parasitic resonances.

III. Antenna Array

Sixteen elements have been placed to form the array at the edge of a mobile terminal PCB (Fig. 5). The total length of the array is 40.13 mm. In order to avoid the appearance of grating lobes, the spacing between elements has been chosen to be $\frac{\lambda_0}{2}$ at 60 GHz, that corresponds to a length of 2.5 mm. Since the unit cell length is 2.63 mm, the adjacent elements are superimposed.

Fig. 5. Geometry of the array.

When the antenna operates at the 60 GHz band, all the elements are active. Nevertheless, at 28 GHz, half-wavelength corresponds to 5.35 mm. Therefore, only the odd elements are

set on. A switch is placed on the even elements of the array to disconnect these antennas at the lower band.

The following subsections detail the behaviour of the antenna array at the different bands.

A. 28 GHz Performance

It is necessary to evaluate how the antennas connected to the switch should be ended. In order to analyse which termination is better, the elements have been grounded, left opened and loaded with 50 Ω and 10 $k\Omega$.

A comparison of the reflection coefficient of the odd elements for each termination of the even antennas is illustrated in Fig. 6. It can be seen that all the ports are matched below -10 dB at 28 GHz for the four choices.

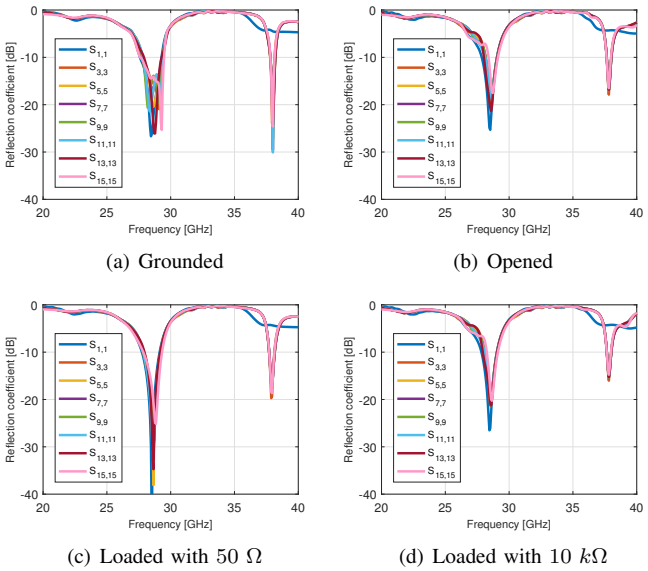

(a) Grounded (b) Opened

(c) Loaded with 50 Ω (d) Loaded with 10 $k\Omega$

Fig. 6. Reflection coefficient of the array for the different terminations.

Since there is no major difference in the reflection coefficient, a comparison of the realized gain of four terminations is shown in Fig. 7 to determine which solution is better. The realized gain definition includes the mismatch loss. The phase-shifts employed to steer the beam are 0°, 45°, 90°, 120° and 180°. The radiation pattern of the grounded and loaded with 50 Ω solutions is flatter for the different scanning angles. In Fig. 7b and Fig. 7d, the realized gain drops at end-fire angles because of the low radiation efficiency.

The total efficiency of an antenna is defined as the ratio of radiated power to stimulated power, which contemplates the reflections at the feeding location. The representation of Fig. 8 is known in statistics as a boxplot. It is a way of depicting the distribution of groups of data through their quartiles. The red horizontal line represents the median value of the distribution (Q_2). The lines extending from the boxes (whiskers) represent the minimum and maximum values of the population. The figure shows that the median value of total efficiency when the non-active antennas are grounded is higher than in the rest options, and the dispersion of the mismatch

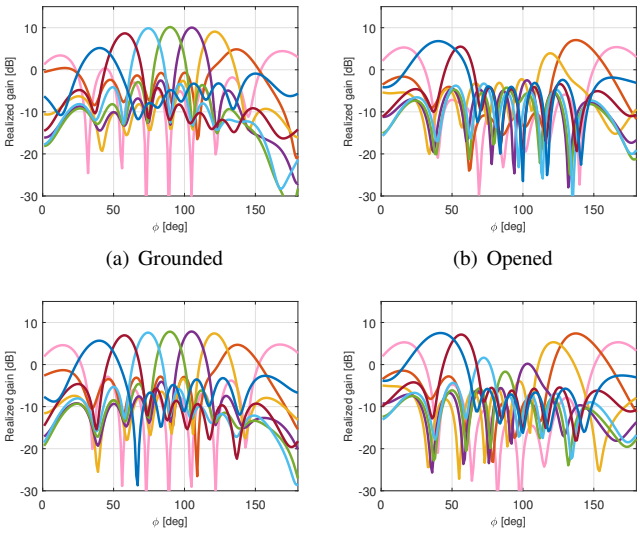

(a) Grounded (b) Opened

(c) Loaded with 50 Ω (d) Loaded with 10 $k\Omega$

Fig. 7. Realized gain termination comparison for different scanning angles.

for the different scanning angles is not as big as in the second and fourth terminations. Therefore, the best performance is obtained when the non-driven elements are grounded.

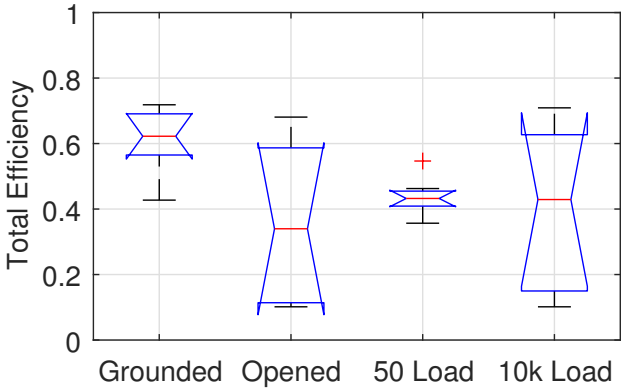

Fig. 8. Total efficiency comparison of the different terminations for the scanning angles at 28 GHz.

B. Parasitic Resonances Performance

As previously discussed, it is necessary that the spacing between elements is shorter than $\lambda/2$ to have end-fire radiation without side lobes. At 38 GHz the maximum spacing corresponds to 3.9 mm, and 3.1 mm at 48 GHz. For this reason, all the elements of the array need to be activated in both scenarios.

Fig. 9 plots the radiation pattern of the array for different scanning angles. The realized gain starts to decrease as the scanning angle gets away from $\phi = 90°$, since the level of the side lobes increases. As it was expected from Fig. 4, the scanning performance at 38 GHz does not have good end-fire radiation.

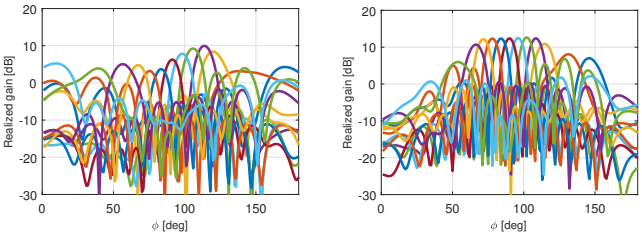

(a) 38 GHz (b) 48 GHz

Fig. 9. Radiation pattern of the array for two parasitic resonances.

C. 60 GHz Performance

At 60 GHz all the elements of the array are active. The high directivity that sixteen elements can reach makes the beam narrow. This allows having more resolution in the scanning and being able to point the beam to a more precise direction. The beam steering for different scanning angles at 60 GHz is represented in Fig. 10. The array is able to scan from end-fire to $\pm 90°$. It can be seen in the plot that the realized gain drops from 15 dB to 10 dB for angles of $\phi \leq 70°$. This behaviour is due to the appearance of side lobes, as illustrated in Fig. 11.

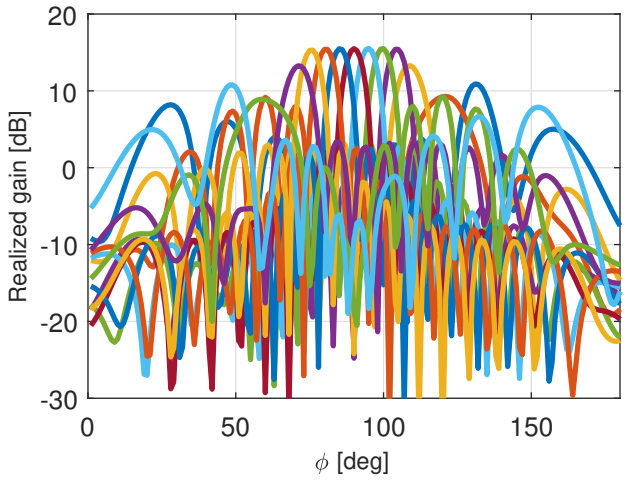

Fig. 10. Realized gain of the antenna for various scanning angles at 60 GHz.

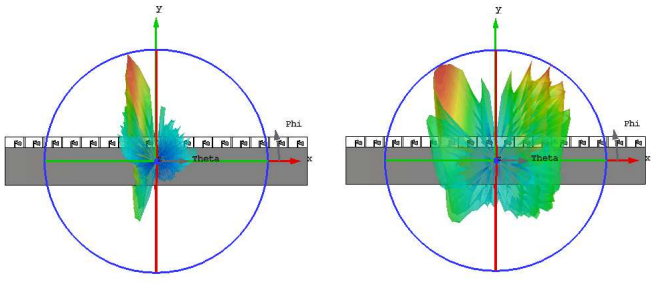

(a) Phase shift of 45° (b) Phase shift of 90°

Fig. 11. Radiation pattern of the 16-element array for two different phase shifts at 60 GHz.

IV. Conclusion

This manuscript proposes a new multi-band bow-tie shaped antenna array for the mm-wave band. Eight elements out of the 16 available are employed in the lowest band to ensure that the coupling between elements is under -10 dB. Simulations show that the best performance is obtained when the non-active elements are grounded.

The array presents good beam-steering characteristics with end-fire radiation at both bands. Furthermore, the antenna is matched over 10 GHz at the upper band.

In conclusion, the low-profile of the designed array and the radiation performance makes it a suitable candidate for mobile terminals of the next generation of communications.

Acknowledgment

The authors would like to thank the WiSpry team for their suggestions on the antenna improvement.

This work is supported by Aalborg University Young Talent Program, and also partially supported by the Innovations-Fonden RANGE project.

References

[1] W. Hong, K.-H. Baek, Y. Lee, Y. Kim, and S.-T. Ko, "Study and prototyping of practically large-scale mmwave antenna systems for 5g cellular devices," *IEEE Communications Magazine*, vol. 52, no. 9, pp. 63–69, 2014.

[2] S. S. Siddiq, G. Karthikeya, T. Tanjavur, and N. Agnihotri, "Microstrip dual band millimeter-wave antenna array for uav applications," in *Microwave, Radar and Wireless Communications (MIKON), 2016 21st International Conference on*. IEEE, 2016, pp. 1–4.

[3] H. Aliakbari, A. Abdipour, R. Mirzavand, A. Costanzo, and P. Mousavi, "A single feed dual-band circularly polarized millimeter-wave antenna for 5g communication," in *Antennas and Propagation (EuCAP), 2016 10th European Conference on*. IEEE, 2016, pp. 1–5.

[4] N. Fokos, "Dual band, dual polarization array antenna for mm-wave radio," Master's thesis, Chalmers University of Technology, 2017.

[5] A. Dadgarpour, B. Zarghooni, T. A. Denidni, and A. A. Kishk, "Dual-band radiation tilting endfire antenna for wlan applications," *IEEE Antennas and Wireless Propagation Letters*, vol. 15, pp. 1466–1469, 2016.

[6] C. A. Balanis, *Antenna theory, analysis and design*, 3rd ed. John Wiley & Sons, 2005.